Comparative Critical Mass Calculations for NNL and ENDF/B-VIII.0 Zirconium Hydride Thermal Neutron Scattering Laws

J. L. Wormald[1*], J. C. Holmes[1], and M. L. Zerkle[1]

[1] Naval Nuclear Laboratory

PO Box 79, West Mifflin, PA 15122-0079, USA

jonathan.wormald@unnpp.gov, jesse.holmes@unnpp.gov, michael.zerkle@unnpp.gov

doi.org/10.13182/PHYSOR22-37586

ABSTRACT

Zirconium hydride (ZrH_x) is a moderator material for TRIGA reactors and historical space reactor systems, such as SNAP-10A. Thermal neutron scattering laws (TSL) for two phases of this material, δ and ε, have been previously evaluated by Naval Nuclear Laboratory (NNL) and submitted to the National Nuclear Data Center (NNDC) for inclusion in the US national ENDF/B-VIII.1 nuclear data library. In contrast to the current ENDF/B-VIII.0 TSL evaluations, which consider only a single phase, the new evaluations are derived from separate *ab initio* calculations for both phases and include coherent elastic effects of the zirconium sublattice. To estimate the impact of these changes to the TSL evaluation of this material, comparative critical mass calculations were performed with MC21 for homogenous mixtures of high-enriched uranium (HEU) and ZrH_x in bare and water reflected sphere configurations. These calculations yield an impact on the estimated critical mass as a function of ^{235}U loading density with maximum differences as large as 1% - 5% for over-moderated thermal spectrum systems. Consequently, the NNL TSL evaluations are anticipated to have a small impact on criticality calculations of thermal reactor systems regardless of the material phase. Nevertheless, characteristic differences exist in the predicted thermal spectra as function of energy for the two sets of TSL evaluations, which are attributed to difference in the underlying phonon density of states of hydrogen bound in ZrH_x.

KEYWORDS: Zirconium hydride, Thermal Scattering Law, Naval Nuclear Laboratory

1. INTRODUCTION

Zirconium hydride (ZrH_x) is a moderator material used in TRIGA reactor fuel [1,2] and has historically been used in other reactors requiring high hydrogen density, including space reactor systems such as SNAP-10A [3]. ZrH_x exist in multiple phases across a range of hydrogen content. The most significant phases for neutron moderation are δ and ε, which are the primary constituents of TRIGA and SNAP-10A fuel systems, respectively [1-3]. At room temperature, δ-ZrH_x is dominant stable phase for $1.56 < x < 1.64$ and exists

* Corresponding author

as a mixed phase with α-Zirconium metal below this range [4]. The ε phase is dominant for $x > 1.74$ and has been proposed to form a mixed phase with the δ phase for $1.64 < x < 1.74$ [4]. In the thermal energy range neutron energy change due to inelastic scattering exhibits a regular structure of quantum oscillations due to the effect of chemical binding of hydrogen in the ZrH_x crystal structure, which differs from relatively featureless, continuum spectra observed in other moderator materials [5]. This behavior greatly influences neutron thermalization and is responsible for the large prompt negative fuel temperature feedback coefficient in TRIGA reactors [5].

Neutron transport calculations (e.g., Monte Carlo) of thermal neutron driven reactors utilize data derived from Evaluated Nuclear Data File (ENDF) thermal scattering law (TSL) evaluations to capture the effect of crystal binding on neutron thermalization. Previously, TSL evaluations were generated with the Full Law Scattering System Hub (FLASSH) [6] for hydrogen and zirconium bound in δ-ZrH_x (H(ZrH_x) and Zr(ZrH_x)) as well as ε-ZrH_2 (H(ZrH_2) and Zr(ZrH_2)) [7]. Subsequently, these evaluations were submitted to NNDC for inclusion in the ENDF/B-VIII.1 nuclear data library. In contrast to the ENDF/B-VIII.0 TSL evaluations that considered ZrH_x as a single phase and neglected any effects from coherent elastic scattering [8], the NNL evaluations consider the two phases explicitly and include the corresponding coherent elastic scattering for the zirconium sublattice in the δ-ZrH_x and ε-ZrH_2 crystal structures. The new NNL TSL evaluations are considered extensible across the entire stoichiometry range of this material. Moreover, the underlying *ab initio* phonon spectra – the fundamental input to TSL generation – of the NNL evaluations were found to have improved agreement with experiment for both phases in comparison to the General Atomics ZrH_x phonon model used in ENDF/B-VIII.0 [7,9].

In this work, critical mass calculations for homogenous mixtures of HEU and ZrH_x were performed as preliminary integral tests of the NNL TSLs for both material phases. These calculations provide an assessment of the impact of differences in the NNL and ENDF/B-VIII.0 TSL evaluations on criticality calculations.

2. COMPUTATIONAL METHODS

MC21 was used to calculate the critical mass for homogeneous mixtures of HEU and ZrH_x in both bare and water (H_2O) reflected sphere configurations. $ZrH_{1.6}$ and ZrH_2 were examined for δ-ZrH_x and ε-ZrH_2, respectively. A standard HEU isotopic composition was used with a total uranium density of 18.82342 g/cm^3. The δ-$ZrH_{1.6}$ and ε-ZrH_2 phases were modeled with room temperature densities of 5.655 g/cm^3 and 5.621 g/cm^3, respectively [10,11]. The H_2O reflector thickness was set to 20 cm and the density of H_2O was set to 0.9981 g/cm^3 corresponding to 1 atm pressure at 293.6 K [12]. Each MC21 simulation was run with 10^6 particles per batch for 200 active and 40 discard batches, which is sufficient to converge k_{eff} to within approximately ± 0.0001 Δk (95% confidence interval). ENDF/B-VIII.0 cross sections and the H-H_2O TSL evaluation were used for all MC21 simulations [13]. Both NNL and ENDF/B-VIII.0 TSL evaluations for ZrH_x were examined. Critical radius searches were performed with a 0.001 Δk convergence criterion.

Nuclear data was prepared for Monte Carlo simulations in MC21 using the NDEX nuclear data processing code [14]. The direct method is used in MC21 to sample thermal neutron scattering outcomes [15]. Oscillations in the ZrH_x inelastic cross sections within the thermal neutron energy range have been shown to be captured with fine resolution using the adaptive energy grid routine in NDEX [16]. The fine incident neutron energy grid generated with the adaptive energy grid method reduces biases in the prediction of k_{eff} for metal hydrides (e.g., ZrH_x) that occur due to interpolation between secondary energy distributions on coarser energy grids [16].

3. RESULTS AND DISCUSSION

The critical mass for homogenous mixtures of HEU and ZrH_x for a range of ^{235}U loading densities are shown in Figure 1, for both a bare sphere and a H_2O reflected sphere configuration. These calculations are based on the NNL TSL evaluations for the δ-ZrH_x and ε-ZrH_2 phases. Critical mass is lower for ε-ZrH_2 relative to δ-$ZrH_{1.6}$ due to the higher hydrogen content; however, in both cases H_2O reflection decreases the minimum critical mass by a factor of nearly 1.5 – 1.7. The fractional change in the critical mass between NNL and ENDF/B-VIII.0 ZrH_x TSL evaluations was computed as,

$$\frac{\Delta M}{M} = \frac{M_{NNL} - M_{VIII}}{M_{VIII}}, \tag{1}$$

where M is the critical mass and the subscript identifies the evaluation version. The magnitude of the change in critical mass was found to be similar for the bare and H_2O reflected configurations for both $ZrH_{1.6}$ and ZrH_2. Although, the change in critical mass between different evaluation versions is generally small, the magnitude of the difference increases as the ^{235}U loading density decreases, as illustrated in the inset to Figure 1(a). For ^{235}U loading densities less than 0.04 g/cm^3 (the over-moderated region) the difference in critical mass exceeds 1 % – 5 %. This fissile loading density range in δ-$ZrH_{1.6}$ is below the ^{235}U loading density of TRIGA fuel systems using both HEU and high assay LEU (HALEU), typically 0.1 – 1 g/cm^3, such that a minimal impact of TSL selection on criticality can be anticipated for this type of fuel system.

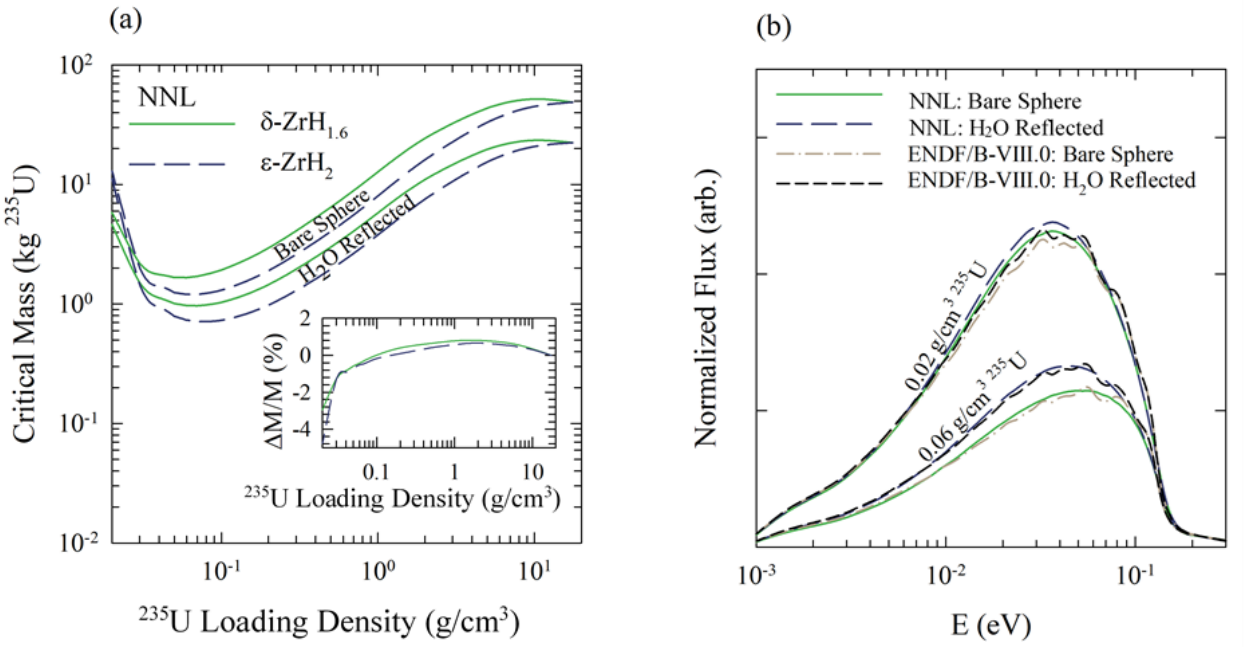

Figure 1. (a) Critical mass of homogenous mixtures of HEU and ZrH_x (both as δ-$ZrH_{1.6}$ and ε-ZrH_2) as a function of ^{235}U loading density for bare and H_2O reflected spheres. The inset illustrates the difference in the predicted critical mass between the ENDF/B-VIII.0 and NNL TSL evaluations for both material phases, as computed with Eq. (1). (b) The thermal flux distribution for $ZrH_{1.6}$ is illustrated for both the bare and H_2O reflected spheres at select ^{235}U loading densities using both the ENDF/B-VIII.0 and NNL ZrH_x TSL evaluations.

Nonetheless, the behavior of $\Delta M/M$ can be related the neutron flux as a function of energy. Thermal flux spectra for both the NNL and ENDF/B-VIII.0 δ-$ZrH_{1.6}$ calculations are provided in Figure 1b for the bare and water reflected configurations. The neutron flux spectra ε-ZrH_2 was found to be similar to δ-$ZrH_{1.6}$. Given the simple spherical geometry and the strong dependence of the total integrated scattering cross section on hydrogen [7], the crystal binding of the hydrogen bound in ZrH_x TSL is the primary driver for differences in the predicted critical mass. For ^{235}U loading densities near 0.06 g/cm^3, both TSL versions of the ZrH_x yield similar neutron flux distributions, consistent with the corresponding small magnitude of $\Delta M/M$. The difference in magnitude of the thermal flux for the bare and water reflected spheres reflects the increased moderations of the reflector at 0.06 g/cm^3. At 0.02 g/cm^3 the thermal flux for bare and water reflect spheres begins to converge. However, the spectra for ENDF/B-VIII.0 is slightly hardened relative to NNL due to additional structure near the peak of the thermal flux. The origin of this structure in ENDF/B-VIII.0 is still to be determined, but may be an artifact of the TSL evaluation methodology.

The differences in critical mass behavior are driven by differences in the secondary energy distributions of the TSLs, as illustrated in Figure 2. The probability of high energy upscattering (~0.15 eV) is less for NNL H(ZrH_x) and H(ZrH_2) at incident energies near 0.0253 eV when compared to ENDF/B-VIII.0 H(ZrH). The increased probability of low neutron energy transfer scattering for the NNL evaluations is also observed for epithermal neutrons (e.g., 1 eV). The effect is a slight reduction in the probability of upscattering as illustrated in Figure 2b. Additionally, the oscillations in the secondary energy distributions for the NNL evaluations are broadened and slightly offset relative to ENDF/B-VIII.0.

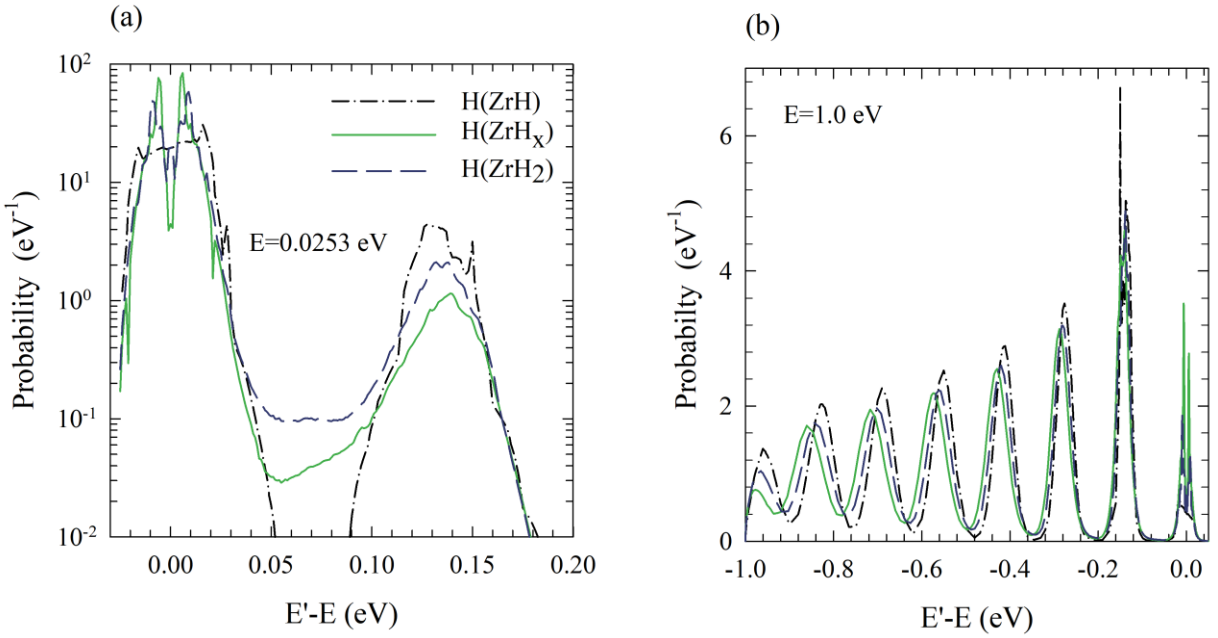

Figure 2. Comparison of the secondary neutron energy distributions for the ENDF/B-VIII.1 H(ZrH_x) and H(ZrH_2) to the ENDF/B-VIII.0 at 0.0253 eV and 1.0 eV. The incident neutron energy is represented as E and the scattered neutron energy is represented as E'.

4. CONCLUSIONS

Criticality calculations to assess the impact of the NNL H(ZrH_x), Zr(ZrH_x), H(ZrH_2), Zr(ZrH_2) TSL evaluations on criticality in comparison to the existing ENDF/B-VIII.0 H(ZrH) and Zr(ZrH) evaluations

have been performed using MC21. Small differences in the critical mass for homogenous mixtures of HEU and ZrH_x for a range of ^{235}U loading densities indicate that use of the NNL evaluations relative to the current ENDF/B-VIII.0 evaluation is likely to have minimal impact on k_{eff} for most ZrH_x moderated systems. Within the simple spherical geometries of the present calculations, changes in the treatment of hydrogen crystal binding in ZrH_x is identified to be the primary driver of differences in predicted criticality rather than inclusion of coherent elastic scattering in $Zr(ZrH_x)$ and $Zr(ZrH_2)$; however, further testing is needed for more complex reactor geometries. Additional integral validation of the NNL TSL evaluations is in progress and will include TRIGA reactor models available in the ICSBEP Handbook [17].

ACKNOWLEDGMENTS

The submitted manuscript has been authored by contractors of the US Government under contract No. DOE-89233018CNR000004. Accordingly, the US Government retains a non-exclusive, royalty-free license to publish or reproduce the published form of this contribution, or allow others to do so, for US Government purposes.

REFERENCES

1. M. T. Simnad, "The U-ZrH_x Alloy: Its Properties and Use in TRIGA Fuel," *Nuclear Engineering and Design*, **64**, pp. 403-422 (1981).
2. G. B West, et al., "Kinetic Behavior of TRIGA Reactors," GA-7882, General Atomics (1967).
3. A.F. Lillie, et al., "Zirconium Hydride Fuel Element Performance Characteristics," AI-AEC-13084, Atomics International Division (1973).
4. E. Zuzek, et al., "The H-Zr (Hydrogen-Zirconium) System," *Bulletin of Alloy Phase Diagrams*, 11, pp. 385-395 (1990).
5. W. L. Whittemore, "Neutron Interactions in Zirconium Hydride," GA-4490, General Atomics (1964).
6. Y. Zhu and A. I. Hawari, "Full Law Analysis Scattering System Hub (FLASSH)," *Proceedings of PHYSOR 2018*, Can´cun, Mexico, April 22-26 (2018).
7. J. L. Wormald, J. C. Holmes, and M. L. Zerkle, "Generation of the TSL for Zirconium Hydrides Using Ab Initio Methods," *Journal of Nuclear Engineering*, **2** (2), pp. 105-113 (2021).
8. R. E. MacFarlane, "New Thermal Neutron Scattering Files for ENDF/B-VI Release 2," LA-12639-MS, Los Alamos National Lab (1994).
9. E. L. Slaggie, "Central force lattice dynamical model for zirconium hydride," *J. Phys. Chem. Solids*, **29**, pp. 923-934 (1968).
10. C. P. Kempter, R. O. Elliot and K. A. Gschneider Jr., "Thermal expansion of delta and epsilon zirconium hydrides," J. Chem. Phys., 33, pp. 837-840 (1960).
11. S. Yamanaka, et al. "Thermal and Mechanical Properties of Zirconium Hydride," *J. Alloys Compd.*, **293-295**, pp. 23-29 (1999).
12. D. A. Brown, et al., "ENDF/B-VIII.0: The 8th major release of the nuclear reaction data library with CIELO-project cross sections, new standards and thermal scattering data," *Nucl. Data Sheets*, **148**, pp. 1-142 (2018).
13. W. Wagner, and A. Pruss, "The IAPWS Formulation 1995 for the Thermodynamic Properties of Ordinary Water Substance for General and Scientific Use," *J. Phys. Chem. Ref. Data*, **31** (2), pp. 387-535 (2002).
14. D. P. Griesheimer, et al. "MC21 v6.0 – A continuous-energy Monte Carlo Particle Transport Code with Integrated Reactor Feedback Capabilities," *Ann. Nucl. Energy* **82**, pp. 29-40 (2015).
15. C. T. Ballinger, "The direct S(α,β) method for thermal neutron scattering," *Proc. Int. Conf. on Math. and Comp. React. Phys. and Environ. Anal.*, Portland, Oregon, (1995).
16. J. L. Wormald, J. T. Thompson and T. H. Trumbull, "Implementation of an Adaptive Energy Grid Routine in NDEX for the Processing of Thermal Neutron Scattering Cross Sections," *Ann. Nucl. Energy*, **149**, pp. 107773 (2020).

17. "International Handbook of Evaluated Criticality Safety Benchmark Experiments," NEA/NSC/DOC(95)03, Nuclear Energy Agency, Organization for Economic Co-operation and Development, Paris, France (2020).